

## Assessment of the future thermal conditions over Europe based on CMIP5 ensemble of agro-meteorological indices

Hristo Chervenkov\* and Kiril Slavov

National Institute of Meteorology and Hydrology (NIMH), 1784 Sofia, Bulgaria

\*Corresponding author: [Hristo.Chervenkov@meteo.bg](mailto:Hristo.Chervenkov@meteo.bg)

### Abstract

Chervenkov, H. & Slavov, K. (2022). Assessment of the future thermal conditions over Europe based on CMIP5 ensemble of agro-meteorological indices. *Bulg. J. Agric. Sci.*, 28 (6), 972–984

Agriculture and forestry are arguably the sectors most dependent on climate and the ongoing and expected future climate changes have essential importance for both of them. Based on the availability of reliable sources of information, which represent CMIP5 global climate change simulations, we present an updated assessment of projected future climate over Europe. The study exploits a set of 5 climate indices with primary relevance for the agriculture and forestry, with special focus on the onset, termination and length of the growing season.

The indices are calculated in consistent manner in the frames of the Global Agriculture project, stored in the database of the Inter Sectoral Impact Model Intercomparison Project and are available on the Copernicus Data Store. As a part of the present study they are systematically analyzed for the near past climate (1981–2010) as well as for the projected future climate up to the end of the 21st century. The projected future climate is evaluated by purpose-build multimodel ensemble from all available models within the project CMIP5 and is performed for all four RCP scenarios.

First of all, the study demonstrates distinct warming expressed in the spatial patterns and the temporal evolution of all considered indicators. In particular, in the scenario with the strongest forcing (RCP8.5) the multiyear mean of the onset of the growing season over Central Europe for the period 2070–2099 becomes 20 days earlier and the termination - 20 days later in comparison to the baseline period, which results in prolongation of the growing season with more than a month. The warming dominates practically over the whole domain, intensifies gradually with the increasing radiative forcing and is statistically significant over its essential part in the most cases. The proposed and applied novel approach for estimation of the timing of the growing season does not reveal statistically significant long-term seasonal shift.

**Keywords:** Agro-meteorological Indices; Growing Season Length; CMIP5 Ensemble; RCPs; Future Climate; Seasonal Shift

### Introduction

Food security is a fundamental precondition for human well-being and the agricultural and food sector is of major economic importance. Agriculture and forestry are arguably the sectors most dependent on climate. The production of both sectors is highly dependent on weather conditions, and extreme weather events beyond the normal conditions experienced by crops can have a dramatic impact on their

yield (Harkness et al., 2020; Hatfield & Prueger 2011, 2015). Changes in the weather conditions may also have adverse effects, causing development of thermophilic weeds, pests, or the emergence of new plant diseases (Luo, 2011; Szyga-Pluta & Tomczyk, 2019). When coinciding with sensitive stages of crop development, unfavorable weather events such as late frost, heavy precipitation, extreme heat, and drought can severely reduce crop yield and affect its quality. Extreme cases of prolonged heat stress or drought can also lead to a

total crop failure (Harkness et al., 2020). The assessment of the frequency of the future occurrence of adverse weather events can, particularly at a large scale, be challenging due to their often localized nature, uncertainty in future projections (Beniston et al., 2007; Seneviratne et al., 2012; Turner & Meyer, 2011) and nonnegligible inter-model spread (Giorgi et al., 2004; Orłowsky & Seneviratne, 2012).

In the recent decades several projects and, consequently, many studies are dedicated on the climate projections over Europe and the Mediterranean basin. The consolidated outcomes from the decade-old fifth phase of the Coupled Model Intercomparison Project (CMIP5) (Taylor et al., 2012) already generally agree on warming in all seasons in Europe during this century, while precipitation projections are more variable across different parts of Europe and seasons (Orłowsky & Seneviratne, 2012; Sillmann et al., 2013). There are still many uncertainties in the magnitude of the expected changes, annual and seasonal variability as well as areal distributions (Dai, 2013; Orłowsky & Seneviratne, 2012; Seneviratne et al., 2012).

The various aspects of the linkage of weather conditions and climate on the one hand and the phenological crop development on the other are subjects of interest in increasing number of recent studies (Barlow et al., 2015; Harding et al., 2015; Harkness et al., 2020; Hatfield & Prueger, 2011) and references therein). The projected future changes of the thermal growing season (TGS) and relevant implications for wheat production over Northern Eurasia at 1.5°C and 2°C global warming and their differences are investigated under RCP4.5 and RCP8.5 scenarios in (Zhou et al., 2018). This study is based on CMIP5 multi-model ensemble and reveals essential prolongation and intensification of the TGS under both RCPs and warming levels, with their magnitude noticeably larger in the 2°C warmer world. The prolonged TGS is attributed to both the earlier onset and later termination of TGSs, with the latter account for the main part. The projections for the duration and degree days of the TGS in Europe derived from CMIP5 multi-model output are comprehensively addressed in (Ruosteenoja et al., 2016). Key message from this study is that in the next decades years with a degree days below the recent past (1971–2000) mean become very uncommon. In the majority of years the degree days count will exceed the 10-year or even the 20- or 50-year return level derived from recent past data.

The present work is dedicated on the assessment of the spatial patterns and as well as the trend estimation of the temporal evolution of five climate indices (CIs) with special focus on the growing season length (GSL) over Europe for the period 1981–2099. Although with primary agro-meteorological importance, the parameters considered here are

common measures with wider application, in particular sensitive indicators for climate change.

The paper is structured as follows: Concise description of the CMIP5 emission scenarios, the primary source of the input data as well as the used models are in 1. Short information of the considered indices is in 2. The core of the article is in 3 where the performed calculations and the obtained results are explained and discussed. As short conclusion remark as well as outlook for further continuation is placed in 4.

## **CMIP5 Scenarios, Models and Input Data**

CMIP5 utilizes a set of emission scenarios referred to as Representative Concentration Pathways (RCPs) (Moss et al., 2010; Van Vuuren et al., 2011). These are based on radiative forcing trajectories and are named according to the forcing level at 2100. There are four RCPs: 2.6, 4.5, 6.0, and 8.5, with the numbers representing the 2100 radiative forcing increase relative to pre-industrial levels in  $\text{W}\cdot\text{m}^{-2}$  (Sun et al., 2015). The peak-and-decline RCP2.6 scenario is designed to meet the 2°C global average warming target compared to pre-industrial conditions (Van Vuuren et al., 2011). The 2100 atmospheric concentration of greenhouse gases (GHG,  $\text{CO}_2$ -equivalent) ranges from 421 ppm for RCP2.6, 650 ppm for RCP4.5, 850 ppm for RCP6.0, to 1370 ppm for RCP8.5 (Van Vuuren et al., 2011). It is worth emphasizing that RCP8.5 assumes radiative forcing levels continue rising after year 2100, RCP6.0 and RCP4.5 assume radiative forcing levels have stabilized in 2100, and RCP2.6 assumes the forcing level peaks before 2100 and then declines.

The CIs considered in this study are part of the database of the Inter Sectoral Impact Model Intercomparison Project (ISIMIP 1, <https://www.isimip.org/protocol/>), Fast Track simulation round, available on the Copernicus Data Store (CDS). ISIMIP was designed as a framework to assess the impacts of climate change in different sectors and at different scales (Schellnhuber et al., 2014). This project used consistent climate and socio-economic input data to multiple impact models (Ito et al., 2020). The core product of the ISIMIP is an open archive which contains collection of 26 climate variables produced from the bias-corrected (BC) output of 5 CMIP5 GCMs according Table 1.

The database spans over the period 1950–2099 (historical run up to 2005), downscaled to a  $0.5^\circ \times 0.5^\circ$  lat-lon grid and covers the global land area. The BC method applied in ISIMIP preserves the absolute changes in monthly temperature, the relative changes in monthly values of precipitation and the other variables and represents a modification of the transfer function approach. Correction of the monthly mean

**Table 1. Fast Track CMIP5 GCMs Considered in ISIMIP**

Model Acronym	Institution	Spat. Resolution (Lon×Lat~ Lev.)
GFDL-ESM2M	Geophysical Fluid Dynamics Lab., USA	144×90L24
HadGEM2-ES	Met Office Hadley Centre, UK	192×145L40
IPSL-CM5A-LR	Institut Pierre-Simon Laplace, France	96×96L39
MIROC-ESM-CHEM	AORI, NIES, JAMSTEC, Japan	128×64L80(T42)
NorESM1-M	Norwegian Climate Centre, Norway	144×96L26

is followed by correction of the daily variability about the monthly mean (Hempel et al., 2013). It is worth mentioning that this method is trend-preserving and the produced long-term means are well represented. The consideration of BC-output is the main methodological difference with our previous works as, for example, (Chervenkov & Slavov, 2021) and similar studies of other groups (Orlowsky & Seneviratne, 2012; Sillmann et al., 2013). It is worth noting, however, that the last two comprehensive studies rely on ensembles prepared with significantly bigger number of models.

The majority of the indicators, included in the ISIMIP-database are computed according the definitions of the Expert Team on Climate Change Detection and Indices (ETCCDI) (Zhang et al., 2011) which makes them universal. They have been calculated for the complete matrix of 5 GCMs×4 RCPs combinations. In addition, as a proxy for historical observations, the 'Watch Forcing Data methodology applied to ERA-Interim (WFDEI)' (Weedon et al., 2014) were used to generate observational historical agroclimatic indicators. This subset is available in the CDS at the same spatial resolution of ISIMIP climate datasets, covers the time range of 1979 to 2013 and its 30 year-long part 1981–2010 (baseline period) is used in the present study as a reference for the current climate.

## Considered Indices

The air temperature is the primary environmental factor affecting the growth, development and yields of crops especially the rate of development (Hatfield & Prueger, 2011; Luo, 2011). Higher temperatures are expected in generally warmer future climate change and the potential for more extreme temperature events could impact plant productivity. All five indices considered in the present study are based on the daily mean or minimum/maximum temperatures, noted further traditionally as  $t_g$ ,  $t_n$  and  $t_x$ .

The accumulative impact of  $t_g$  on phenological crop development could be quantified by various agro-meteorological (AM) indices (Seemann et al, 1979). Similarly to other sector-oriented indicators which do not have internationally

agreed definitions, the computation of some of the AM indices can be performed in different ways, depending on the available data, region of interest, nature and scope of the study (Harding et al., 2015). A certain exception is the GSL which is standardized in frames of collaborative initiatives like European Climate Assessment & Dataset (ECA&D) project (van Engelen et al., 2008) and ETCCDI (Zhang et al., 2011). The main reason is its primary importance which makes it probably the most recognizable AM index of all. According the unified definition of ECA&D and ETCCDI, the GSL is the annual count between first span of at least 6 days with  $t_g > 5^\circ\text{C}$  and first span after July 1 (in Northern Hemisphere) of at least 6 days with  $t_g < 5^\circ\text{C}$  (Zhang et al., 2011, Zhou et al., 2018). The units of measurement of the GSL are, obviously, days. Although some alternative definitions, respectively calculation methods, exists (Linderholm, 2006; Ruosteenoja et al., 2016), we will follow strictly the ECA&D and ETCCDI one.

Primarily due to its popularity, the growing season is subject of many studies, considering the regional and global climate (Mesterhazy et al., 2018; Ruosteenoja et al., 2016 and detailed list in Linderholm, 2006), whereas little attention is paid on its onset day of year (DOY) and termination DOY, noted further DOYB and DOYC respectively. The lack could be explained partially with that the most standardized software tools for computation of CIs outputs only GSL and not DOYB/DOYC. Data for these two parameters is also not present in the ISIMIP Fast Track database. Changes in the timing and length of the GSL, however, may not only have essential relevance for plant and animal ecosystems, but persistent increases in GSL may lead to long-term increases in carbon storage and changes in vegetation cover which may affect the climate system (Linderholm, 2006; Zhou et al., 2018). The relative importance of DOYB and DOYC is the main our motivator to estimate and, subsequently, assess them in a similar way to the rest of CIs in this study as it will be shown in the next section.

The modelling of frost risk is complex as the damage depends on the crop variety, planting and harvest dates as well as many other factors. In addition to temperature, the duration of freezing temperatures is important in determining the

damage that occurs. The longer the duration the greater the chance of ice-nucleation occurring, and the greater spread of ice-nucleation through the ear and subsequent plant damage (Barlow et al., 2015). The thermal impact of prolonged frost episodes can be assessed in feasible way with the climate index of consecutive frost days (CFD). The CFD, known also as cold spell, is defined as the largest number of consecutive days where  $t_n < 0^\circ\text{C}$ . The CFD is most meaningful for temperate climate and frequently used as a general frost damage indicator.

The adverse effects of the heat on the phenological plant development are manifold and, similarly to the impact of the frost, depend greatly on the variety of the species. Most generally, under heat stress conditions plants must divert resources from growth towards coping strategies (Barlow et al., 2015; Harding et al., 2015). This study, however, does not consider these impacts in more detail as the focus is on the heat stress climatology. In the CIs-based approach the prolonged heat stress is quantified with the index maximum number of consecutive summer days (CSU). The CSU, known also as hot spell, is defined as the largest number of consecutive days where  $t_x > 25^\circ\text{C}$ . Similarly to the CFD, the CSU is ECA&D index (Van Engelen et al., 2008); it is calculated on seasonal basis and expressed in days. The CSU is used, beside its other applications, as information provider on heat stress impact on the growth for C4 crops (e.g. maize).

The index of warm and wet days (WW) is the single one compound indicator, from the ones considered here; hence it depends on temperature and precipitation sum, rather than the daily mean and/or extreme temperature solely. The WW is based on the Beniston's concept for heat and moisture quantiles (Beniston, 2009) and is defined as the number of days where  $t_g > t_{g75}$  and  $RR > RR_{75}$ . Here RR is the daily precipitation amount at a wet day (i.e. days with precipitation  $> 1.0$  mm);  $t_{g75}$  and  $RR_{75}$  are the calendar day 75<sup>th</sup> percentiles of the daily mean temperature and the daily precipitation sum calculated according the ETCCDI definition (Zhang et al., 2011). The WW provides an indication concerning the crop development, especially leaf formation. It is also informative of occurrence of various pests' insects and especially fungi. Unlike the CFD and CSU, the WW imply percentile based, rather than absolute threshold. It is measured in days.

The Biologically Effective Degree Days (BEDD) index has been specifically targeted to describe grape growth (Gladstones, 1992). The BEDD index is based on a growing degree days concept and is calculated by:

$$BEDD = \sum_{i=01.04}^{i=30.09} \min \left[ \max \left( \frac{t_{g_i}}{2} - t_l, 0 \right), t_h - t_l \right], \quad (1)$$

where  $t_h = 30^\circ\text{C}$  and  $t_l = 10^\circ\text{C}$  are the upper and lower threshold temperature respectively. The units of measurement of the BEDD are degree days which will be noted henceforth as  $^\circ\text{D}$ . The BEDD is a measure for the accumulated heat during the warm period of the year. It determines crop development stages/rates — crop development will decelerate/accelerate below and above certain threshold limits.

Total degree days, threshold temperatures, as well as ranges for GSL, have been established for many crops (Barlow et al., 2015; Linderholm, 2006; Luo, 2011). These methods of expressing crop heat requirements are widely used for agricultural climate evaluation in the former Soviet Union, Bulgaria, Poland, Romania, and a number of other countries (Seemann et al., 1979) which motivates their selection in this study.

## Calculations and Results

### Estimation of the GSL Onset and Termination

The finest temporal resolution that is commonly used in the climatology for generating CIs is one month. To have a better indication, however, when crop emergence, flowering, etc., takes places (given the provided weather data series) the temporal resolution should be finer than one month. Due to this reason 18 from all 26 indicators, including  $t_g$ , are stored in the ISIMIP database for 10 day periods (also known as 'decades'). Hence the models in Table 1 use 360-day long year, every year contains 36 records. These time series give the opportunity to estimate the onset and termination day of the GSL effectively.

In the past many attempts are documented to estimate the DOYB and DOYC from temperature data on monthly, even longer basis. Most of them are motivated by the absence of data with daily temporal resolution which hampers the straightforward calculation of the DOYB and DOYC, respectively the GSL according the definition in Section 2. The formulas, used in (Szyga-Pluta & Tomczyk, 2019) on monthly data and modified from us for decadal resolution, are as follows:

$$DOYB = 10(i-1) + 5.5 + 10 \frac{t_b - t_{g_i}}{t_{g_{i+1}} - t_{g_i}} \quad (2)$$

$$DOYC = 180 + 10(i-1) + 5.5 + 10 \frac{t_{g_i} - t_b}{t_{g_i} - t_{g_{i+1}}} \quad (3)$$

The index  $i$  in Equation 2 denotes the number of the interval ( $i = 1$ -first,  $i = 18$ -last, i.e. in the first half of the year) were the first upwards transition through the threshold  $t_b = 5^\circ\text{C}$  occurs. Respectively, the index  $i$  in Equation 3 denotes the interval with the first downwards transition through the threshold in the second half of the year.

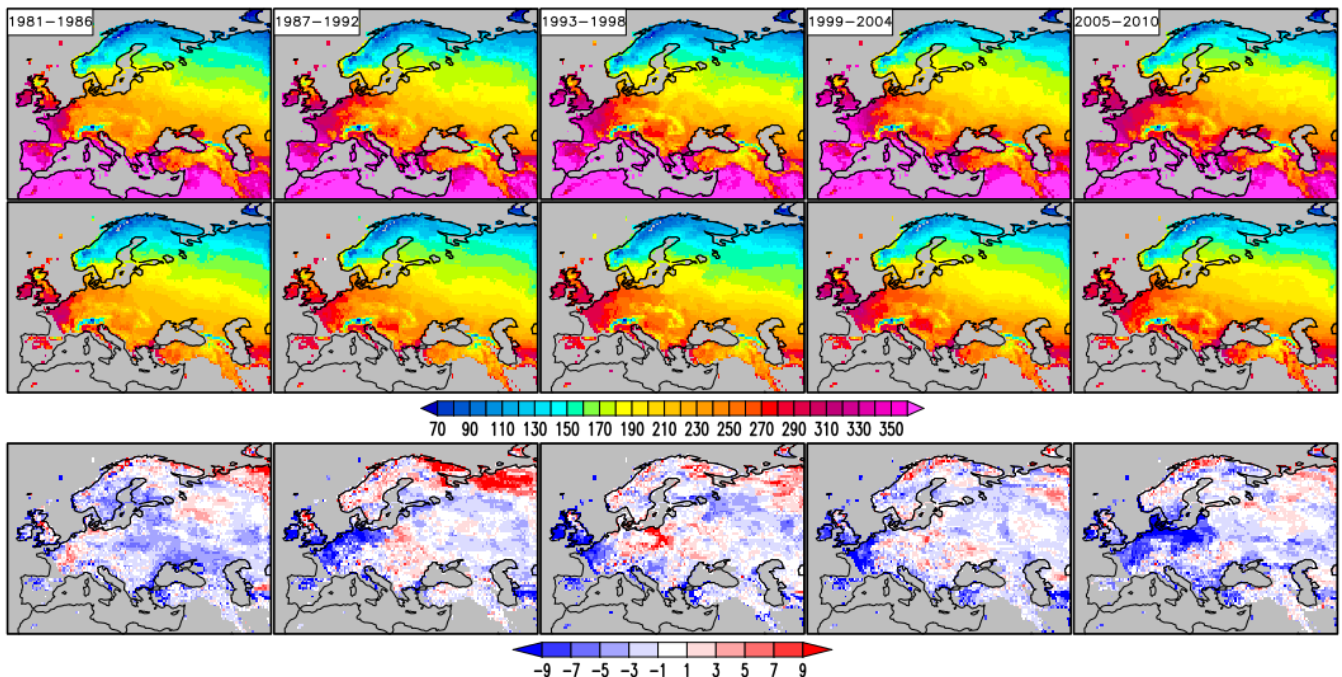


**Fig. 1. Reference and calculated GSL (units: days) in the first and second row correspondingly for the considered intervals. The relative bias (in %) is shown on the third row**

The method, which is linear interpolation indeed, suppose the presence of at least one upward transition in the first and at least one transition downwards in the second half of the year. If this condition is not satisfied, the DOYB, DOYC and subsequently GSL, can not be calculated following the definition in Section 2. Thus, in particular, if the  $t_g$  is below or above  $t_b$  in all 36 intervals we will not set  $GSL=0$  or  $GSL=360$  correspondingly.

The next step, in order to check the applicability of this method, is to compare the results for the GSL obtained with Equations 2 and 3 with independent data. As a reference we use the GSL for the baseline period 1981–2010. The temporal means of the GSL for the five 6 years long intervals 1981–1986, 1987–1992, 1993–1998, 1999–2004, 2005–2010 from the reference and these, obtained from the  $t_g$  for the same time spans as well as the relative bias between them are shown in Figure 1.

The most apparent difference between the reference and calculated GSL is the smaller spatial coverage of the second one. Due to the reason stated above, in the regions with a vegetation period all year long as Northern Africa, the Iberian Peninsula, Southern France and almost all Mediterranean islands, the DOYB and DOYC could be not calculated. Second, which is most important, is that the magnitude of the relative bias is small. Over the bigger part of the domain it is between -3% and 3% without evident systematic patterns. The estimation of the agreement between the calculated GSL and reference can be quantified also with the root mean square error (RMSE) and comparison of the time series of the area-weighted averages (AA) (over all definite grid cells) as shown in Figure 2.

Figure 2 shows that the RMSE over the larger part of the domain is smaller than a week; The AA-series of the calcu-

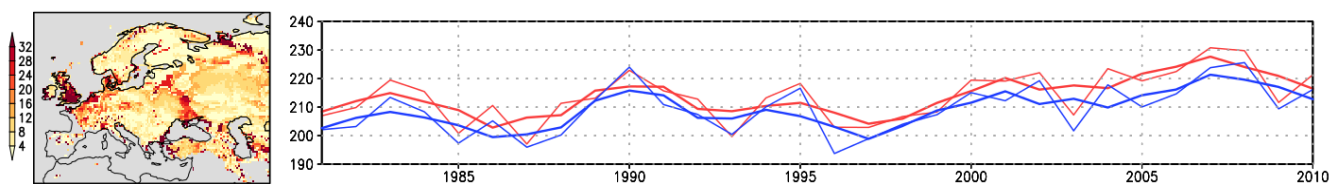


**Fig. 2. Left pane: RMSE of the calculated GSL (units: days); Right pane: Time series of the AA of the reference (red line) and calculated GSL (blue line). The running 3-year means are shown with fat lines**

lated GSL systematically underestimates the reference with almost constant value which is smaller than 10 days.

Finally we can conclude that, according to the results of the performed evaluation, the proposed method for calculation of the DOYB and DOYC is feasible enough and acceptable from the point of view its accuracy.

**Ensemble Spatial Patterns and Temporal Evolution**

This subsection describes concisely the performed calculations step by step and outlines the results regarding the spatial patterns of the considered CIs as well as their temporal evolution in the projected future climate.

First, the necessary data are downloaded from the CDS using purpose-bulid python scripts. After that all ISIMIP-data sets are significantly post-processed and the most essential stages are:

- The data sets for each model and RCP which are down-loadable in 30-year time slices are merged in common data streams for 2011–2099.
- The indices with equal temporal resolution are joined in common netCDF4 files.
- Multi-model (MM) ensemble statistics as multi-model mean (MMM), MM 25<sup>th</sup>, 50<sup>th</sup> and 75<sup>th</sup> percentiles which are often referred as lower quantile, median and upper quantile and traditionally noted as X25, X50 and X75 are computed.
- Due to the particular region of interest and storage constrains only a spatial subset over Europe and adjacent areas is stored.

All netCDF manipulations are performed with the powerful tool Climate Data Operators (<https://code.zmaw.de/projects/cdo>). Additionally, for the current study only, all of the considered indices are aggregated by time on annual basis.

The present study concerns only the MM ensemble statistics rather than the simulation output of the individual models. This type of analysis weights all models equally. Although an equal weighting does not incorporate known differences among models in their ability to reproduce various climatic conditions, a number of research studies (Herger et al., 2018; Knutti, 2010; Overland et al., 2011) have found that the MMM with equal weighting is superior to any single model in reproducing the present-day climate.

The uncertainty range identified from the five ISIMIP-GCMs listed in Table 1 was investigated in detail in (McSweeney & Jones, 2016), indicating that the subset covers more of the uncertainty in the temperature and precipitation changes projected by 36 CMIP5 GCMs than other randomly sampled five-GCM subsets. The ability of the ISIMIP model ensemble subset to reproduce the observed temperature and

precipitation and how this subset captures the uncertainty in projected change compared with the full CMIP5 ensemble set was comprehensively studied in (Ito et al., 2020). One of the key findings in (Ito et al., 2020) is that the spreads of the bias and Taylor’s skill score from the ISIMIP-subset is smaller than those obtained from the full set of CMIP5 ensemble for the annual mean temperature and precipitation. Compared with the random samples, the ISIMIP subset shows high coverage for the temperature change in all regions and, by contrast, low coverage for the precipitation change in more than 60% of the regions. Although it is not clear whether the globally consistent subset adequately represents the regional climate phenomena, the outcomes from theses two studies are methodological ground to select the ISIMIP-database. This is reasonable, in the same time pragmatic choice, comparing with the studies (Ruosteenoja et al., 2016; Zhou et al., 2018) which are based also on CMIP5 ensembles but with much more members. It is also worth emphasizing that the ISIMIP-archive has been successfully used recently in the regional climate studies (Chervenkov et al., 2020a; 2020b).

Our analysis is focused on the MM median (MMX50), as in (Sillmann et al., 2013) which, in contrast to the MMM is statistically robust and thus much less sensitive to outliers in the ensemble. The inter-model spread is estimated with the interquartile range (the difference X75-X25).

The analysis starts with the indicators connected with the growing sea-season. Hence it is essential to assess not only the GSL but also its timing, we consider the middle day of the growing season (DOYM), where  $DOYM = (DOYB+DOYC)/2$  as simple indicator of the seasonal shift. Lets suppose that in projected future (generally warmer) climate the growing season will starts  $\Delta_1$  days earlier and ends  $\Delta_2$  later in comparison to the reference. Then the DOYM in the future period will be:

$$\begin{aligned}
 DOYM_F &= \frac{DOYB_R - \Delta_1 + DOYC_R + \Delta_2}{2} = \\
 &= DOYM_R + \frac{\Delta_2 - \Delta_1}{2}, \tag{4}
 \end{aligned}$$

where the indices F and R denotes the future and reference periods correspondingly. Obviously  $DOYM_F > DOYM_R$  if  $\Delta_1 < \Delta_2$ ;  $DOYM_F = DOYM_R$  if  $\Delta_1 = \Delta_2$  and  $DOYM_F < DOYM_R$  if  $\Delta_1 > \Delta_2$  and thus the shift of DOYM towards earlier/later DOY indicates seasonal shift of the entire growing season, independently from the total GSL itself.

Figure 3 shows the comparison of the spatial patterns of the multiyear means of the DOYB, DOYM, DOYC and GSL for the reference period (noted REF) with the MM ensemble

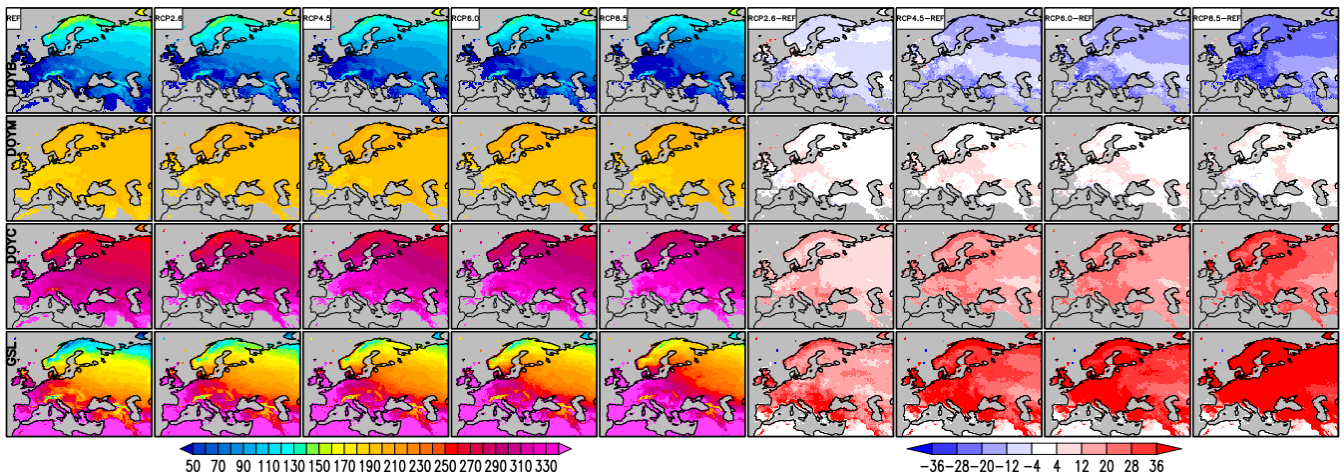


**Fig. 3. Multiyear means of the DOYB, DOYM, DOYC and GSL for the reference period, multiyear means of the MMX50s of these indicators for the future period as well as absolute changes of the future values relative to the reference. The units are DOYs for DOYB, DOYM, DOYC and days for GSL**

medians of these indicators for the future period (i.e. 2070–2099) for all 4 scenarios. The DOYB, DOYM and DOYC plotted in Figure 3 are computed from the MMX50s of the  $t_g$  for each RCP according to Equation 2 and 3 and subsequently averaged in time. The results for the GSL are the ensemble medians composed from the available data sets in the ISIMIP Fast Track database.

The most apparent result for DOYB, DOYM and DOYC is that the spatial extent vary from the reference to the projected future and from RCP to RCP. This is a direct consequence of the accepted and explained method for calculation of these indicators in Subsection 3.1. Hence the  $t_g$  in the future is generally changed towards warmer climate, more and more territories become with mean daily temperatures above the threshold of  $5^\circ\text{C}$  in the whole year. The climate change signal (i.e. the absolute differences between the future and reference periods) is expressed in gradual decrease of DOYB and increase of the DOYC and GSL from RCP2.6 to RCP8.5, which is generally proportional to the radiative forcing. Thus,

in the scenario with the strongest forcing (RCP8.5) the DOYB is over Central Europe 20 days smaller and the DOYC - 20 days greater in comparison to the reference, which results in prolongation of the GSL with more than a month. The climate change signal is without a clear spatial structure. The DOYM in the future do not shows any distinguishable difference to the reference under any scenario, suggesting absence of principal change of the timing of the GSL.

We will assess the continuous temporal evolution of the considered indicators analyzing the time series of their areal averages (AAs). The AA of the GSL is shown in Figure 4.

The most notable result is the steady increase of the GSL for all scenarios and with lapse proportional to the radiative forcing. It could be seen also that the interquartile model spread remain practically overlapping for all RCPs until the middle of the 21st century.

The projected spatial patterns of the CFD, CSU, WW and BEDD as well as their differences relative to the reference period are shown in Figure 5.

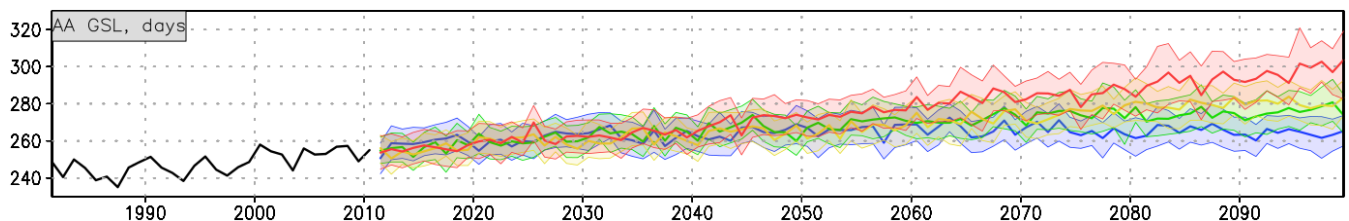


**Fig. 4. AA of the GSL for the reference (solid black line) and simulated by the CMIP5 ensemble for the RCP2.6 (blue), RCP4.5 (green), RCP6.0 (yellow) and RCP8.5 (red). Solid lines indicate the ensemble MMX50 and the shading, respectively the thin lines, indicates the interquartile ensemble spread (MMX25 to MMX75)**

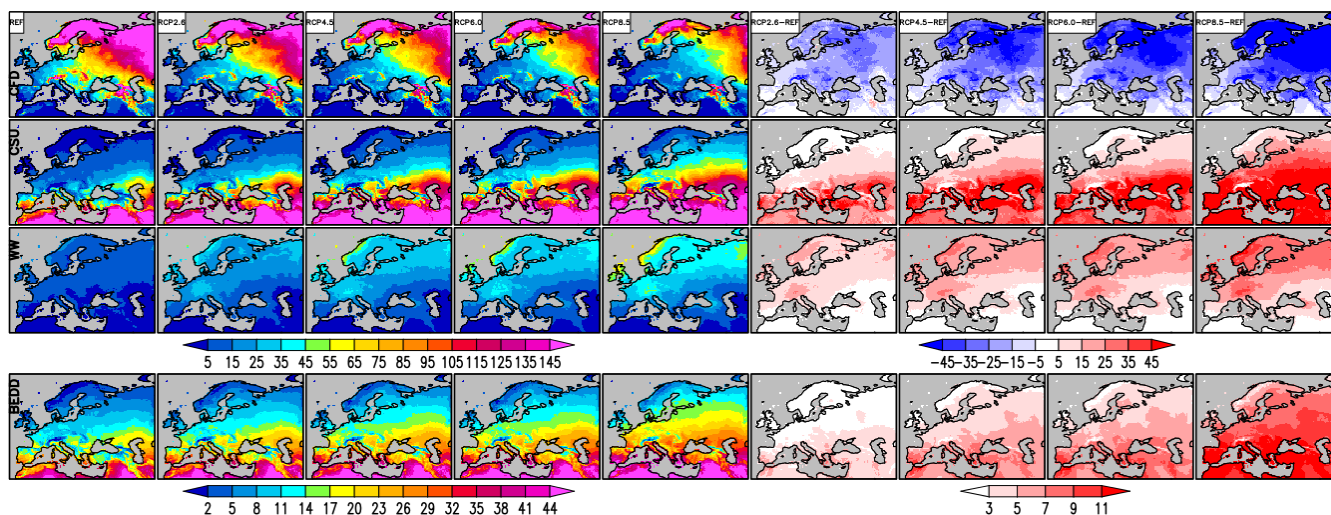


Fig. 5. Same as Fig. 3, but for CFD, CSU, WW and BEDD. The units for CFD, CSU, WW are days, and for BEDD – 100°D°

The fields of these indices have clear spatial structure: continental gradient from southwest to northeast for CSU, from north to south for CSU and BEDD and from south to north for WW. It is worth emphasizing that the gradient for the WW is almost absent in the reference period but becomes stronger in the future with the increase of the radiative forc-

ing. The strengthening of the continental gradient in the projected future could be linked with irregular warming. It is emphasized in (Sillmann et al., 2013) that the strongest warming generally occurs in the interior of the continents, in this case over Eastern and Northeastern Europe. The CFD is close to zero along the Mediterranean and Atlantic coast-

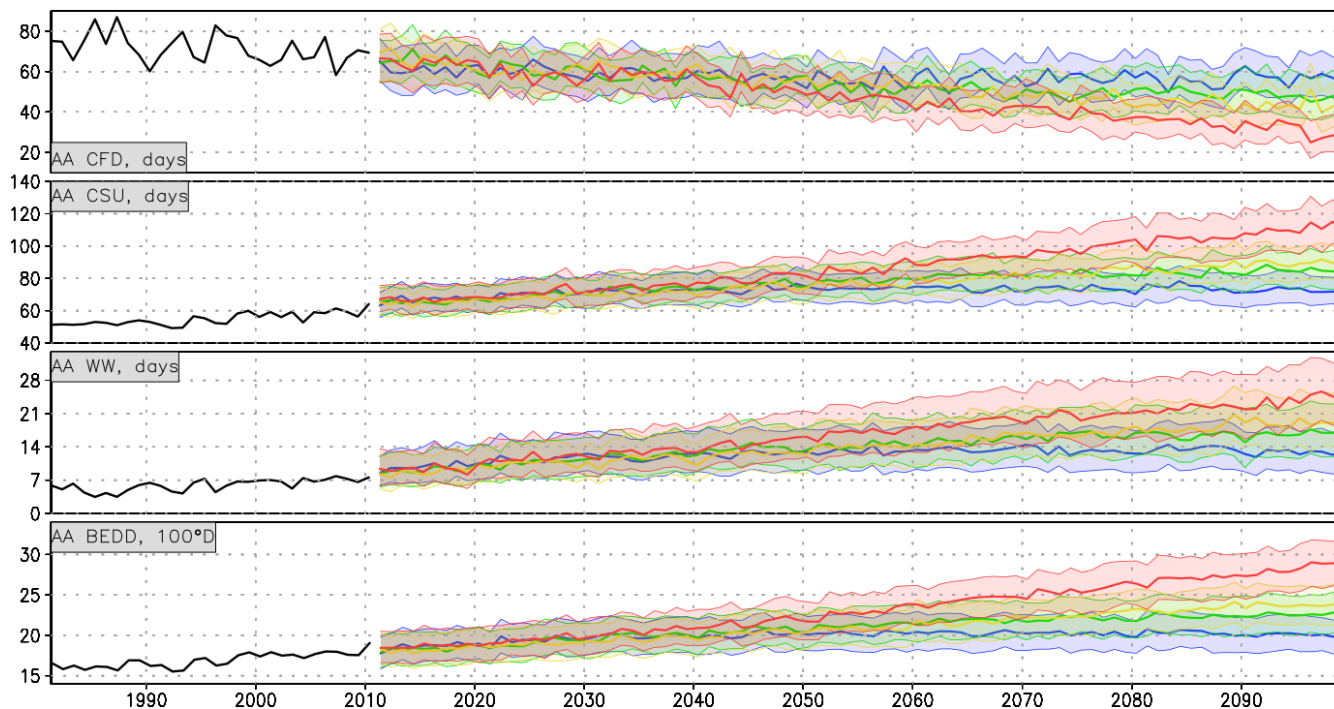


Fig. 6. Same as Fig. 4, but for CFD, CSU, WW and BEDD according the subplot titles

lines and over the Iberian, Apennine Peninsulas and other big regions as the western half of France. The maximum of the CFD is in northeast where the continentality of the climate is most prominent. Similarly to the long-term change of the GSL, shown in Figure 3, the overall picture is consistent with the general change of  $t_n$ ,  $t_g$  and  $t_x$  over the region: gradual decrease of CFD and increase of CSU, and BEDD. The amount of warming by scenario, expressed in the terms of these indices, generally ranges from high to low as follows: RCP8.5, RCP6.0, RCP4.5 and RCP2.6.

The temporal evolution of the AAs of the CFD, CSU, WW and BEDD are shown in Figure 6.

As expected, there is a consistent decrease of CFD and increase of CSU, WW and BEDD. Similarly to the GSL, the

projected changes are smallest for the weaker RCP2.6 scenario and vice versa. Similarly to the case of the GSL, the interquartile model spread remains practically overlapping for all RCPs until the middle of the 21<sup>st</sup> century.

#### Trend Analysis

The importance of assessing trends of any key variables is often emphasized in the modern climatology and, subsequently, it is essential part of many recent studies (Beniston, 2009; Chervenkov & Slavov, 2019; Orłowsky & Seneviratne, 2012; Sillmann et al., 2013 and references therein).

The magnitude of the trend is estimated with the Theil-Sen Estimator (TSE) (Theil, 1950; Sen, 1968), which is preferably used in many geophysical branches, including

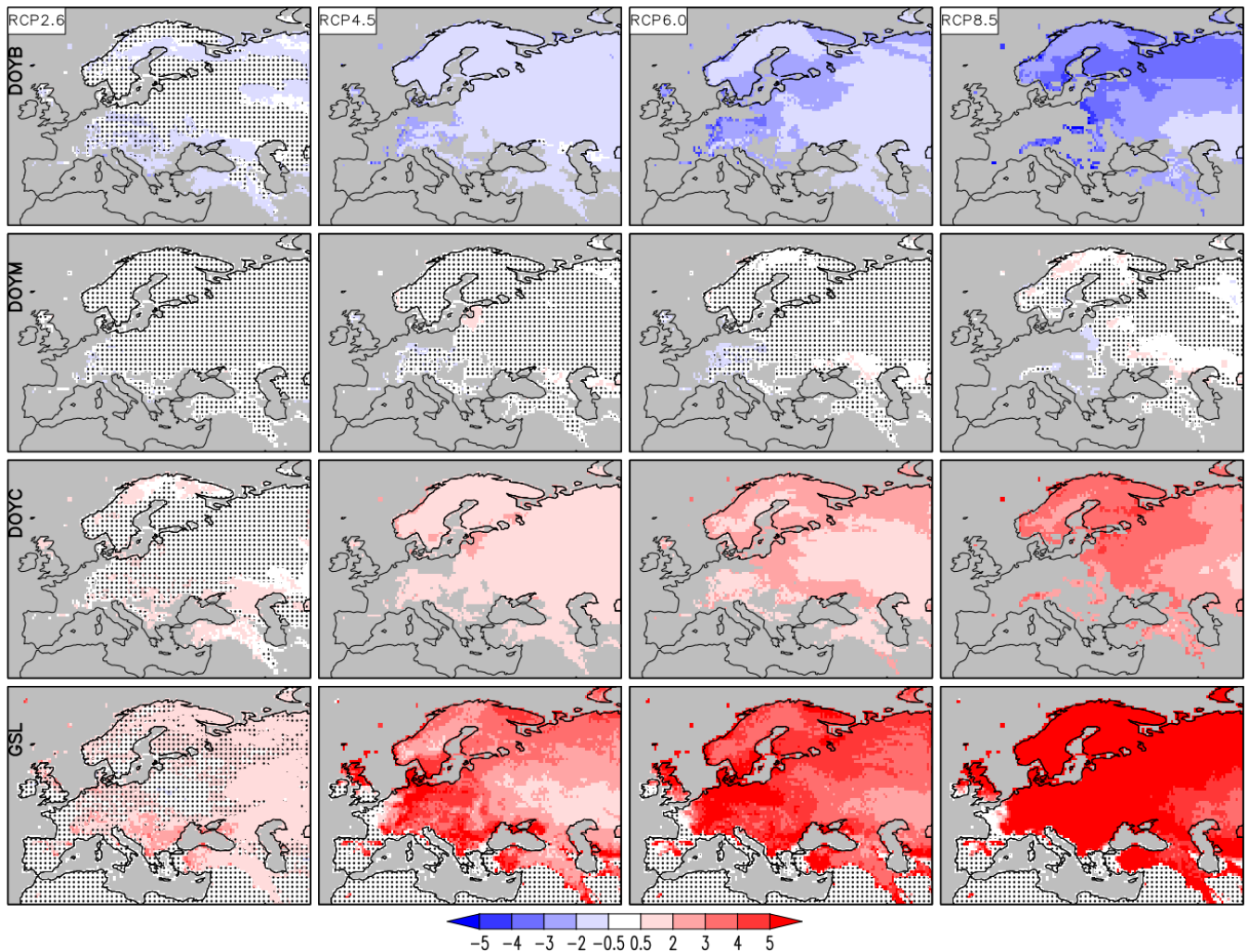


**Fig. 7.** Trend magnitude (units: days/10 yr) of the MMX50s of the DOYB, DOYM, DOYC and GSL. Stippling indicates grid points with changes that are not significant at the 5% significance level

climatology. The statistical significance is analyzed with the non-parametric Mann-Kendall (MK) test (Kendall, 1938; Mann, 1945). As the TSE, The MK test is a rank-based procedure, especially suitable for non-normally distributed data, data containing outliers and nonlinear trends. The both methods are practically standard tools for trend analysis in climatology. In the present study they are applied to every grid point time series and each scenario separately, but only if all values are definite.

The results from the trend analysis of the GSL-related measures are shown in Figure 7.

Overall the picture is coherent with the results discussed above: consistent shift of the DOYB towards earlier dates and, vice versa, consistent shift of the DOYC towards later dates.

This effect is strengthening with the radiative forcing, leading to persistent prolongation of the GSL. Under the scenario with the strongest forcing, RCP8.5, the tg rises above the threshold temperature and thus DOYB can not be calculated, respectively trend analysis can not be performed over the bigger part of the domain. The trend of the DOYB and DOYC is significant at the 5% level practically everywhere for all scenarios, except for RCP2.6. Subsequently, the trend significance for the GSL is confirmed for RCP4.5–RCP8.5 over all areas where it is smaller than 360 in the reference period. If the GSL = 360 in the recent conditions, it could not rise further even in warmer climate hence it is bounded above. Thus it remains constant and there is no trend. As expected, there is practically no trend of the DOYM everywhere and under any scenario.

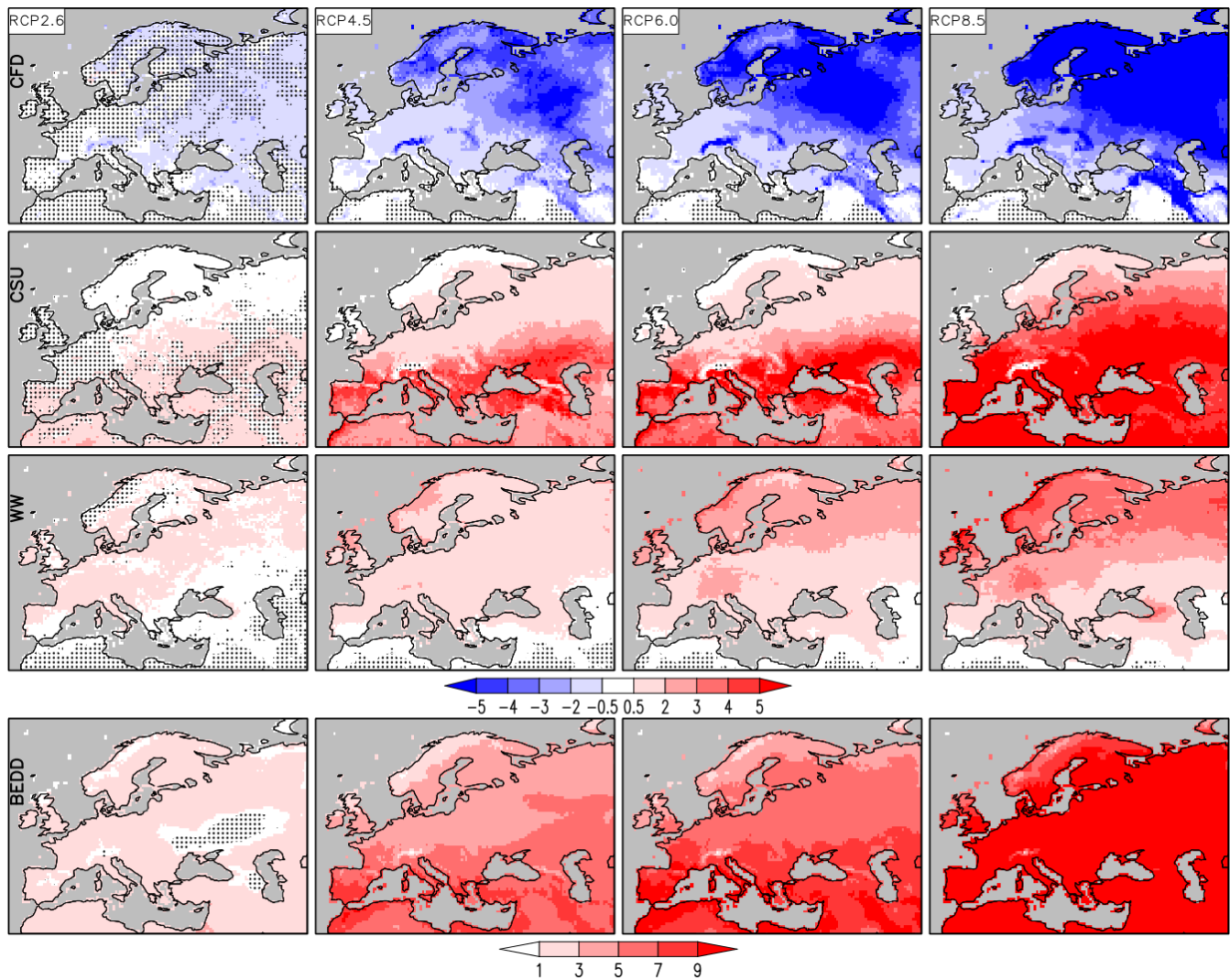


Fig. 8. Same as Fig. 7, but for CFD, CSU, WW (units: days/10 yr) and BEDD (units: °D/yr)

We conclude our assessment with the results from the trend analysis of CFD, CSU, WW and BEDD which are shown in Figure 8.

Generally, these results agree with the outcomes for the GSL-related quantities. It can be seen markedly expressed negative trend of the single ‘cold’ index, the CFD, and clearly emphasized positive trend for CSU, WW and BEDD. The geographical specifics of the trend magnitude patterns are noticeable. The biggest (in absolute values) change rates of the CSU are in northeast, whereas these of the CSU and BEDD — over the southern half of the domain. The fastest increase of the WW is over Northern Europe. The trend of all indicators is statistically significant almost over the whole domain for RCP4.5–RCP8.5; for WW and BEDD even for RCP2.6.

### *Perspective for Bulgaria*

Due to understandable reasons, Bulgaria is in the focus of the authors’ interest.

Southeast Europe, in particular Bulgaria, is part of the Mediterranean basin. The Mediterranean basin lies in a transition zone between the arid climate of North Africa and the temperate and rainy climate of central Europe and it is affected by interactions between mid-latitude and tropical processes (Giorgi et al., 2004). Because of these features, even relatively minor modifications of the general circulation can lead to substantial changes in its climate. This makes the Mediterranean a potentially vulnerable region to climatic changes (Sillmann et al., 2013). More detailed inspection of the generated in this study digital maps, on which are based Figures 3 and 5 reveals the following results for the projected average changes over Bulgaria in respect to the reference period.

The common conclusion from the analysis of the listed in Table 2 values is that, as expected, the projected changes are generally proportional to the radiative forcing. The magnitude of the expected changes is relatively big and, which is more important, they are statistically significant for all scenarios. It is worth mentioning, however, that detailed picture of the regional specifics could be revealed applying regional, rather than global climate models as noted in (Giorgi et al., 2004).

**Table 2. Projected average changes over Bulgaria**

	RCP2.6	RCP4.5	RCP6.0	RCP8.5
GSL, days	30 – 50	40 – 85	40 – 85	50 – 90
CFD, days	-35 – -10	-40 – -10	-45 – -10	-50 – -15
CSU, days	20 – 60	40 – 75	40 – 80	70 – 110
WW, days	3 – 8	5 – 10	7 – 11	8 – 14
BEDD, 100°D	4 – 6	7 – 8	7 – 9	13 – 14

## Conclusion

Based on the availability of reliable sources of information, such as CMIP5 global climate change simulations, we present an updated assessment of projected future climate over Europe. The study exploits a set of climate indices with primary relevance for the agriculture and forestry, stored in the ISIMIP-database which is freely available from the CDS. The indices are calculated in a consistent manner in the frames of the Global Agriculture project and are systematically analyzed for the near past climate (1981–2010) as well as for the projected future climate up to the end of the 21st century.

Although not exhaustive, the study demonstrates, first of all, distinct warming, expressed in the spatial patterns and temporal evolution of all of the considered indicators. Due to the fact that these indicators display the same types of variability as the temperature data on which they are based, they could be regarded as universal climatological measures. The warming dominates practically over the whole domain, intensifying gradually with the increasing radiative forcing (i.e. from RCP2.6 to RCP8.5) and is statistically significant over its essential part in the most cases. It is worth emphasizing that the trend patterns are consistent over the whole domain, i.e., there are no mixed trends for a given index. A certain exception is the trend distribution of the DOYM but, as a whole, it is not spatially significant.

The presence of data-sets with 10 day temporal resolution in the ISIMIP-database appears as a valuable asset with multiple potential benefits. In particular, it allows, as shown in this study, relatively simple but at the same time accurate enough computation of the onset and termination day of the growing season which, in turn, facilitates the estimation of the long-term seasonal shift of the GSL. The general absence of statistically significant shift practically everywhere in Europe is also key message from the present study.

The study could be continued in many aspects. Important issues such as, seasonal variations and detailed regional specifics, have to be focal point in future work. Similar studies could be methodologically reliable scientific basis of the long-range policy and expert assessments for managing systems as the agriculture and forestry.

### Acknowledgements

Hence this study is entirely based on freely available data and software, the authors would like to express their deep gratitude to the primary CMIP5 model output vendors as well as all other organizations and institutions (MPI-M, UNI-DATA, ISMIP, CDS), which provides free of charge software and data. Without their innovative data services and tools this work would be not possible. Personal thanks to I. Tsonevsky from the European Centre for Medium-Range Weather Forecasts for the cooperation.

### References

- Barlow, K. M., Christy, B. P., O'Leary, G. J., Riffkin, P. A. & Nuttall, J. G. (2015). Simulating the impact of extreme heat and frost events on wheat crop production: a review. *Field Crops Res.*, 171, 109–119. <https://doi.org/10.1016/j.fcr.2014.11.010>
- Beniston, M. (2009). Trends in joint quantiles of temperature and precipitation in Europe since 1901 and projected for 2100. *Geophys. Res. Lett.*, 36, L07707. <https://doi.org/10.1029/2008GL037119>
- Beniston, M., Stephenson, D., Christensen, O., Ferro, C., Frei, C., Goyette, S., Halsnaes, K., Holt, T., Jylhä, K., Koffi, B., Palutikof, J., Schöll, R., Semmler, T., & Woth, K. (2007). Future extreme events in European climate: an exploration of regional climate model projections. *Climatic Change*, 81, 71–95. <https://doi.org/10.1007/s10584-006-9226-z>
- Chervenkov, H. & Slavov, K. (2019). Theil-Sen Estimator vs. Ordinary Least Squares - Trend Analysis for Selected ETCCDI Climate Indices. *Compt. Rend. Acad. Bulg. Sci.*, 72 (1), 47–54. <https://doi.org/10.7546/CRABS.2019.01.06>
- Chervenkov, H. & Slavov, K. (2021). ETCCDI Thermal Climate Indices in the CMIP5 Future Climate Projections over Southeast Europe. Proceedings of the 14th Annual Meeting of the Bulgarian Section of SIAM, Studies in Computational Intelligence, (in press).
- Chervenkov, H., Ivanov, V., Gadzhev, G. & Ganey, K. (2020). Assessment of the Future Climate over Southeast Europe Based on CMIP5 Ensemble of Climate Indices - Part One: Concept and Methods. In: Gadzhev G., Dobrinkova, N. (eds). Proceeding of 1st International Conference on Environmental Protection and disaster RISks - Part One, ISBN978-619-7065-38-1 144–156. <https://doi.org/10.48365/envr-2020.1.13>
- Chervenkov, H., Ivanov, V., Gadzhev, G. & Ganey, K. (2020). Assessment of the Future Climate over Southeast Europe Based on CMIP5 Ensemble of Climate Indices - Part Two: Results and Discussion. In: Gadzhev G., Dobrinkova, N. (eds). Proceeding of 1st International Conference on Environmental Protection and disaster RISks - Part One, ISBN978-619-7065-38-1 157–169. <https://doi.org/10.48365/envr-2020.1.14>
- Dai, A. (2013). Increasing drought under global warming in observations and models. *Nature Clim. Change*, 3, 52–58
- Giorgi, F., Bi, X. & Pal, J. (2004). Mean, interannual variability and trends in a regional climate change experiment over Europe. II: climate change scenarios (2071–2100). *Climate Dynamics*, 23, 839–858. <https://doi.org/10.1007/s00382-004-0467-0>
- Gladstones, J. S. (1992). *Viticulture and environment : a study of the effects of environment on grapegrowing and wine qualities, with emphasis on present and future areas for growing winegrapes in Australia*. Adelaide : Winetitles.
- Harding, A. E., Rivington, M., Mineter M. J. & Tett, S. F. B. (2015). Agro-meteorological indices and climate model uncertainty over the UK. *Climatic Change*, 128, 113–126. <https://doi.org/10.1007/s10584-014-1296-8>
- Harkness, C., Semenov, M. A., Areal, F., Senapati, N., Trnka, M. & Balek, Bishop, J. (2020). Adverse weather conditions for UK wheat production under climate change. *Agricultural and Forest Meteorology*, 282-283, 107862. <https://doi.org/10.1016/j.agrformet.2019.107862>
- Hatfield, J. L. & Prueger, J. H. (2011). Agroecology: Implications for Plant Response to Climate Change. In: Crop Adaptation to Climate Change (eds. S. Yadav, R. J. Redden, J. L. Hatfield, H. Lotze-Campen and A. E. Hall), *Wiley-Blackwell*, West Sussex, UK, 27–43.
- Hatfield, J. L., Prueger, J. H. (2015). Temperature extremes: Effect on plant growth and development. *Weather and Climate Extremes*, 10(A), 4–10. <https://doi.org/10.1016/j.wace.2015.08.001>
- Hempel, S., Frieler, K., Warszawski, L., Schewe, J. & Piontek, F. (2013). A trend-preserving bias correction – the ISI-MIP approach. *Earth Syst. Dynam.*, 4, 219–236. <https://doi.org/10.5194/esd-4-219-2013>
- Heger, N., Abramowitz, G., Knutti, R., Angelil, O., Lehmann, Sanderson, B. (2018). Selecting a climate model subset to optimize key ensemble properties. *Earth Syst. Dynam.*, 9, 135–151. <https://doi.org/10.5194/esd-9-135-2018>
- Ito, R., Shiogama, H., Nakaegawa, T. & Takayabu, I. (2020). Uncertainties in climate change projections covered by the ISI-MIP and CORDEX model subsets from CMIP5. *Geosci. Model Dev.*, 13, 859–872. <https://doi.org/10.5194/gmd-13-859-2020>
- Kendall, M. G. (1938). A new measure of rank correlation. *Biometrika*, 30, 1–93.
- Knutti, R. (2010). The end of model democracy? *Climatic Change*, 102, 395–404. <https://doi.org/10.1007/s10584-010-9800-2>
- Linderholm, H. W. (2006). Growing season changes in the last century. *Agric. Forest Meteorol.*, 137, 1–14. <https://doi.org/10.1016/j.agrformet.2006.03.006>
- Luo, Q. (2011). Temperature thresholds and crop production: a review. *Climatic Change* 109, 583–598. <https://doi.org/10.1007/s10584-011-0028-6>
- McSweeney, C. F. & Jones, R. G. (2016). How representative is the spread of climate projections from the 5 CMIP5 GCMs used in ISI-MIP? *Clim. Serv.*, 1, 24–29. <https://doi.org/10.1016/J.CLISER.2016.02.001>
- Mann, H. B. (1945). Nonparametric tests against trend. *Econometrica*, 13, 245–259.
- Mesterhazy, I., Meszaros, R., Pongracz, R., Bodor, P., Ladanyi, M. (2018). The analysis of climatic indicators using different growing season calculation methods – an application to grapevine grown in Hungary. *IDOJARAS*, 122(3), 217–235.
- Moss, R. H., et al. (2010). The next generation of scenarios for climate change research and assessment. *Nature*, 463, 747–756. <https://doi.org/10.1038/nature08823>

- Orlowsky, B. & Seneviratne, S. I.** (2012). Elusive drought: uncertainty in observed trends and short- and long-term CMIP5 projections. *Hydrol. Earth Syst. Sci.*, *17*(5), 1765–1781. <https://doi.org/10.3929/ethz-b-000073994>
- Overland, J. E., Wang, M., Bond, N. A., Walsh, J. E., Kattsov, V. M. & Chapman, W. L.** (2011). Considerations in the selection of global climate models for regional climate projections: The Arctic as a case study. *J. Climate*, *24*, 1583–1597. <https://doi.org/10.1175/2010JCLI3462.1>
- Ruosteenoja, K., Raisanen, J., Venalainen, A. & Kamarainen, M.** (2016). Projections for the duration and degree days of the thermal growing season in Europe derived from CMIP5 model output. *Int. J. Climatol.*, *36*, 3039–3055. <https://doi.org/10.1002/joc.4535>
- Schellnhuber, H. J., Frieler, K. & Kabat, P.** (2014). The elephant, the blind, and the intersectoral intercomparison of climate impacts. *P. Natl. Acad. Sci. USA*, *111*, 3225–3227. <https://doi.org/10.1073/PNAS.1321791111>
- Seemann, J., Chirkov, Y. I., Lomas, J. & Primault, B.** (1979). Agrometeorology. *Springer-Verlag Berlin Heidelberg New York*. <https://doi.org/10.1007/978-3-642-67288-0>
- Sen, P. K.** (1968). Estimates of the regression coefficient based on Kendall's tau. *Journal of the American Statistical Association*, *63*, 1379–1389.
- Seneviratne, S., Nicholls, N., Easterling, D., Goodess, C., Kanae, S., Kossin, J., Luo, Y., Marengo, J., McInnes, K., Rahimi, M., Reichstein, M., Sorteberg, A., Vera, C., Zhang, X.,** (2012). Changes in climate extremes and their impacts on the natural physical environment. In: Field, C.B., Barros, V., Stocker, T. F., Qin, D., Dokken, D.J., Ebi, K. L. (Eds.), *Managing the Risk of Extreme Events and Disasters to Advance Climate Change Adaptation. Special Report of the Intergovernmental Panel on Climate Change. Cambridge University Press, Cambridge, UK, and New York, NY, USA*, 109–230. <https://doi.org/10.1017/CBO9781139177245.006>
- Sillmann, J., Kharin, V. V., Zhang, X., Zwiers, F. W. & Bronaugh, D.** (2013). Climate extremes indices in the CMIP5 multimodel ensemble: Part 2. Future climate projections. *J. Geophys. Res. Atmos.*, *118*, 2473–2493. <https://doi.org/10.1002/jgrd.50188>
- Sun, L., Kunkel, K. E., Stevens, L. E., Buddenberg, A., Dobson, J. G. & Easterling, D. R.** (2015). Regional Surface Climate Conditions in CMIP3 and CMIP5 for the United States: Differences, Similarities, and Implications for the U.S. National Climate Assessment, *NOAA Technical Report NESDIS 144*, 111. <https://doi.org/10.7289/V5RB72KG>
- Szyga-Pluta, K. & Tomczyk, A. M.** (2019). Anomalies in the length of the growing season in Poland in the period 1966–2015. *IDOJARAS*, *123*(3), 391–408. <https://doi.org/10.28974/idojaras.2019.3.8>
- Theil, H.** (1950). A rank-invariant method of linear and polynomial regression analysis. I, II, III, *Nederl. Akad. Wetensch., Proc.*, *53*, 386–392, 521–525, 1397–1412.
- Turner, N. C. & Meyer, R.** (2011). Synthesis of Regional Impacts and Global Agricultural Adjustments. In: *Crop Adaptation to Climate Change* (eds S. S. Yadav, R. J. Redden, J. L. Hatfield, H. Lotze Campen and A. E. Hall). <https://doi.org/10.1002/9780470960929.ch12>
- Taylor, K. E., Stouffer, R. J. & Meehl, G. A.** (2012). An Overview of CMIP5 and the Experiment Design. *Bull. Amer. Meteor. Soc.*, *93*, 485–498. <https://doi.org/10.1175/BAMS-D-11-00094.1>
- Van Engelen, A., Klein Tank, A., van der Schrier, G. & Klok, L.** (2008). European Climate Assessment & Dataset (ECA&D), Report 2008, "Towards an operational system for assessing observed changes in climate extremes". KNMI, De Bilt, The Netherlands, 68.
- Van Vuuren, D. P., Edmonds, J., Kainuma, M., Riahi, K., Thomson, A., Hibbard, K., Hurtt, G., Kram, T., Krey, V., Lamarque, J.-F. Masui, T., Meinshausen, M., Nakicenovic, N., Smith, S. J., Rose, S. K.** (2011). The representative concentration path-ways: An overview, *Clim. Chang.*, *109*, 5–31. <https://doi.org/10.1007/s10584-011-0148-z>
- Weedon, G. P., Balsamo, G., Bellouin, N., Gomes, S., Best, M. J. & Viterbo, P.** (2014). The WFDEI meteorological forcing data set: WATCH Forcing Data methodology applied to ERA-Interim reanalysis data. *Water Resources Research*, *50*(9), 7505–7514.
- Zhang, X., Alexander, L., Hegerl, G. C., Jones, P., Tank, A. K., Peterson, T. C., Trewin, B., Zwiers, F. W.** (2011). Indices for monitoring changes in extremes based on daily temperature and precipitation data. *WIREs Clim Change*, *2*, 851–870. <https://doi.org/10.1002/wcc.147>
- Zhou, B., Zhai, P., Chen, Y. & Yu, R.** (2018). Projected changes of thermal growing season over Northern Eurasia in a 1.5°C and 2°C warming world. *Environ. Res. Lett.*, *13* <https://doi.org/10.1088/1748-9326/aaa6dc>

*Received: December, 18, 2020; Accepted: June, 26, 2021; Published: December, 2022*